Impact of Plasma Shaping on Electron Heat Transport in TCV L-mode Plasmas at Various Collisionalities

Y. Camenen, A. Pochelon, R. Behn, A. Bottino[1], A. Bortolon, S. Coda, A. Karpushov, O. Sauter, G. Zhuang and the TCV team

Ecole Polytechnique Fédérale de Lausanne (EPFL), Centre de Recherches en Physique des Plasmas, Association EURATOM-Confédération Suisse, CH-1015 Lausanne, Switzerland

e-mail contact of main author: yann.camenen@epfl.ch

Abstract. The impact of plasma shaping on electron heat transport is investigated in TCV L-mode plasmas. The study is motivated by the observation of an increase of the energy confinement time with decreasing plasma triangularity that may not be explained by a change in the temperature gradient induced by changes in the geometry of the flux surfaces. The plasma triangularity is varied over a wide range, from positive to negative values, and various plasmas conditions are explored by changing the total electron cyclotron (EC) heating power and the plasma density. The mid-radius electron heat diffusivity is shown to significantly decrease with decreasing triangularities and, for similar plasma conditions, only half of the EC power is required at a triangularity of –0.4 compared to +0.4 to obtain the same temperature profile. Besides, the observed dependence of the electron heat diffusivity on the electron temperature, electron density and effective charge can be grouped in a unique dependence on the plasma effective collisionality. In summary, the electron heat transport level exhibits a continuous decrease with decreasing triangularity and increasing collisionality. Local gyro-fluid and global gyro-kinetic simulations predict that trapped electron modes are the most unstable modes in these EC heated plasmas with an effective collisionality ranging from 0.2 to 1. The modes stability dependence on the plasma triangularity is investigated. For higher effective collisionality, ranging from 1 to 2 and achieved in ohmic plasmas, the experimental electron heat transport is no longer observed to decrease with decreasing triangularity.

1. Introduction

The shape of the plasma cross-section in tokamaks is observed to strongly influence a wide range of plasma properties, such as the plasma pressure and current limits [1] or the sawtooth stability [2, 3]. Active plasma shaping thus offers a way to control these plasma properties and to obtain an improved understanding of the underlying physics. In previous studies, the influence of the plasma shape on the core energy confinement has been investigated using the unique shaping capabilities of the TCV tokamak. These studies were performed in L-mode plasmas to minimize the influence of plasma edge stability.

Ohmic plasmas with line averaged density from 5 to $9\times10^{19}\mathrm{m}^{-3}$ were first considered, with plasma elongation κ and plasma triangularity δ in the range $1<\kappa<1.85$ and $-0.3<\delta<0.55$. The energy confinement time τ_E was observed to significantly increase with the plasma elongation but to be independent of the plasma triangularity [4, 5]. For higher plasma elongation, $2.2<\kappa<2.7$, the energy confinement no longer increased with κ [6]. In these ohmic discharges, the variations of τ_E with plasma shape, including the saturation at high elongation, can be explained by changes in the temperature gradient induced by changes in the geometry of the flux surfaces, without requiring the inclusion of a shape dependence of the transport coefficients [4, 5].

The influence of plasma shape on energy confinement was then investigated in the presence of 1.5MW of central EC heating for a wide range of triangularity, $-0.65<\delta<0.55$, in plasmas of

1. Present address: Max-Planck-Institut für Plasmaphysik, EURATOM Association, D-85748, Germany

intermediate elongation, κ=1.5, and of line averaged density of about 1.8×10^{19}m^{-3}. In contrast to the higher density ohmic case, τ_E depended strongly on the plasma triangularity, scaling as $(1+\delta)^{-0.35}$ [7]. Such a dependence can not be explained by geometrical effects, which has motivated the present study that focusses on the influence of plasma triangularity on core electron heat transport.

The paper is organized as follows: the experiments and analysis methods are described in Section 2, Section 3 compares the core electron heat transport level between two plasmas configurations with a negative and a positive triangularity. The study is then extended to a larger domain in Section 4 that investigates the role of the plasma collisionality and triangularity. To evaluate the potential role of the trapped electron modes (TEM) in the transport of electron heat, the TEM dependence on plasma triangularity is assessed using gyro-kinetic simulations described in Section 5. Finally, some conclusions and comments are presented in Section 6.

2. Experimental set-up

The experiments are performed with L-mode configurations limited on the central column of the torus. The influence of plasma shaping on electron heat transport is investigated by varying the plasma triangularity, $-0.4<\delta<0.4$, while the plasma elongation, κ=1.6, minor radius, a=0.25m, and toroidal magnetic field, B_T=1.44T, are kept constant. The radial electron heat flux Q_e is controlled by depositing 0.45 to 1.8MW of EC heating power slightly off-axis, at ρ=0.4, with the radial coordinate defined by $\rho = \sqrt{V/V_{LCFS}}$, where V is the volume of the flux surface labelled by ρ and V_{LCFS} the volume of the last closed flux surface. The EC power deposition, calculated with the linear ray-tracing code TORAY-GA [8], is strongly radially localized slightly outside the q=1 surface to minimize sawtooth activity [9]. For the explored line averaged densities, ranging from 1 to 2.2×10^{19}m^{-3}, the EC power is fully absorbed in the first pass through the electron cyclotron resonance. There is no current driven by the EC waves as the wave vector is maintained perpendicular to the magnetic field by adjusting the toroidal injection angle for each value of the triangularity. The level of electron heat transport is assessed in steady-state by computing the electron heat diffusivity. The electron heat diffusivity χ_e characterizes the temperature gradient that may be sustained by a given heat flux in specific plasma conditions and is obtained from the power balance:

$$\chi_e = -Q_e \Big/ \left(n_e \langle |\nabla\rho|^2 \rangle \frac{\partial T_e}{\partial \rho} \right)$$

In this expression, the brackets indicate an average over the flux surface. The electron heat flux is calculated taking contributions from the EC heating power, the ohmic power and the electron to ion equipartition power into account. The EC heating power is the main contribution to the electron heat flux with an ohmic heating power never exceeding 0.25MW. Due to the low densities, there is little power transferred from the electrons to the ions and the electron temperature is higher than the ion temperature. The radiated power is <10% of the total heating power and tomographic inversions of bolometric data indicates that >85% of it is radiated from the region ρ>0.7. The radiated power may therefore be neglected in the calculation of the core electron heat diffusivity. The electron temperature and density profiles are measured every 25ms using a Thomson Scattering system and averaged over ~100 confinement times (~300ms) after a stationary internal inductance is obtained. The C^{6+} ion temperature profile is measured by a Charge Exchange Recombination Spectroscopy (CXRS) diagnostic.

3. Electron heat transport comparison at two triangularities

In a first step, two plasmas discharges with triangularity δ=–0.4 and δ=+0.4 are compared. Special care was taken to achieve similar conditions for these discharges. The central line averaged density, $\bar{n}_e = 1.43\times10^{19}\,\mathrm{m}^{-3}$, is kept constant to within ±3% and the EC heating power and the total current are adjusted to obtain similar electron temperature and safety factor profiles. The safety factor profile q is reconstructed using the PRETOR transport code [10] in interpretative mode, accounting for the ohmic and bootstrap contributions to the current profile. The average effective charge is estimated from the neoclassical conductivity assuming a flat effective charge profile and matching the calculated and measured total plasma current.

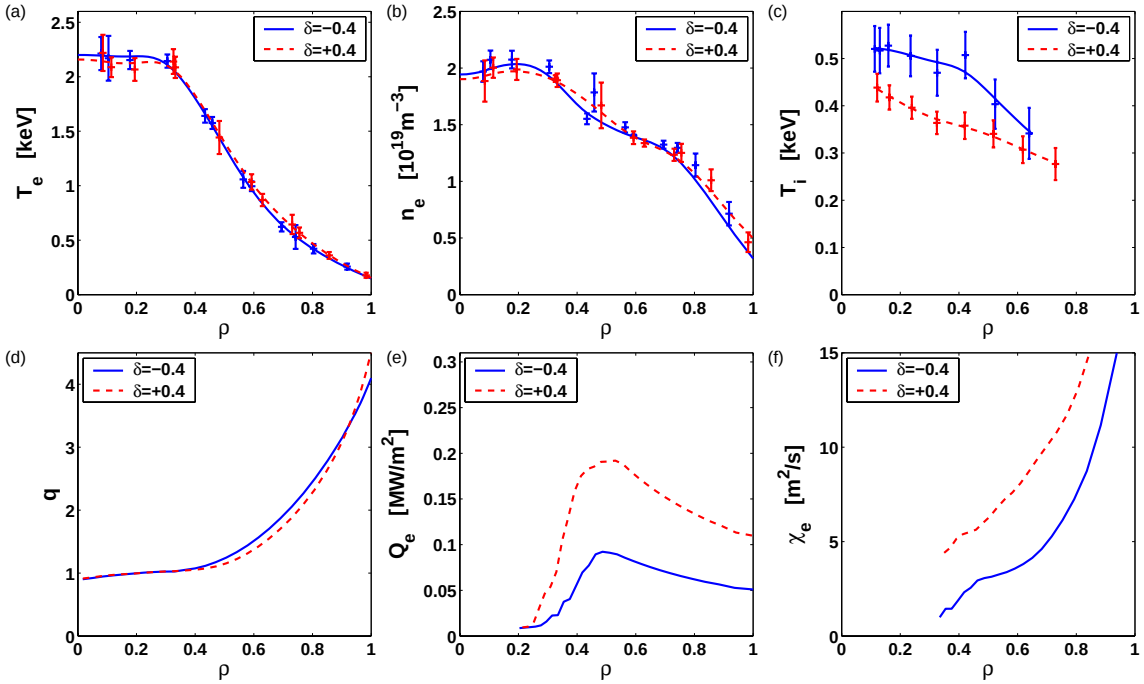

FIG. 1. Comparison of two plasmas with different triangularity δ*, showing that for similar electron temperature (a), electron density (b), ion temperature (c) and safety factor (d) profiles, the electron heat flux (e) and the electron heat diffusivity (f) are halved at* δ=–0.4 *compared to* δ=+0.4.

As shown in FIG. 1, the electron temperature, the electron density and the safety factor profiles are quasi identical, as are the average effective charge values: Z_{eff}=3.5 at δ=–0.4 and Z_{eff}=3.6 at δ=+0.4. It is remarkable that, for such comparable plasma conditions, the electron heat transport is halved at δ=–0.4 compared to δ=+0.4 [11]. The EC heating power required to obtain the same temperature profile was only 0.58MW at δ=–0.4 compared to 1.26MW at δ=+0.4. As the EC heating power dominates the power balance, the electron heat flux and the electron heat diffusivity are consequently halved at δ=–0.4 compared to δ=+0.4. The ion heat transport is also reduced with decreasing triangularities. As shown in FIG. 1, the ion temperature is higher at δ=–0.4 than at δ=+0.4 while the ion heating power, dominated by electron-ion collisions, is constant.

The term $\langle|\nabla\rho|^2\rangle$, involved in the calculation of the transport coefficients and representing the average flux surface compression, remains approximately constant, see FIG. 2. Even for a constant pressure profile, the Shafranov shift is, however, highly influenced by the change in plasma triangularity and could be, at least in part, responsible for the change of χ_e. As illustrated in FIG. 2, the Shafranov shift increases with decreasing triangularity by 2cm, i.e. ~8%

of the minor radius, between these two discharges. The small difference in the plasma current, I_p=260kA at δ=–0.4 and I_p=285kA at δ=+0.4, required to produce the same q=1 surface radius, does not significantly influence the electron heat transport, as demonstrated in Section 4. The strong reduction of the electron heat transport observed over the whole plasma is mirrored by an increase of the electron energy confinement time from 3.9 to 8.1ms.

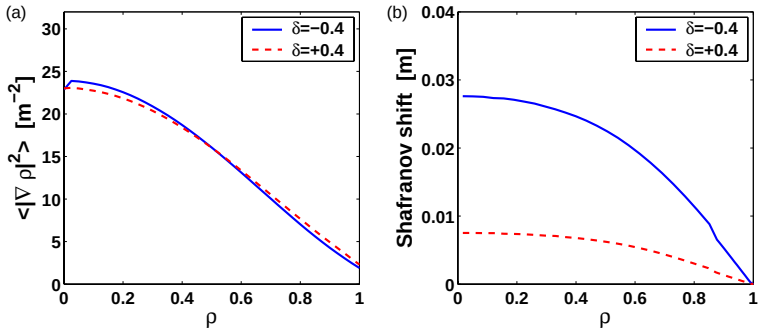

FIG. 2. Variation of $\langle|\nabla\rho|^2\rangle$ *(a) and of the Shafranov shift (b) profiles with the plasma triangularity. While the average flux surface compression is not affected by a triangularity change, the Shafranov shift strongly increases with decreasing triangularity.*

4. Impact of collisionality and triangularity on electron heat transport

To confirm the impact of plasma triangularity on electron heat transport over a larger range of plasmas conditions, the plasma triangularity is now varied from δ=–0.4 to δ=+0.4 and various plasmas densities and EC power levels are explored, whilst keeping the EC power deposition radius constant at ρ=0.4. The plasma current is slightly varied, 240<I_p<290kA, to assess the influence of the safety factor profile variation in the triangularity scan. The plasma parameters domain covered at mid-radius for T_e, n_e, Z_{eff}, T_i, ν_{eff}, R/L_{T_e}, R/L_{n_e}, T_e/T_i, R/L_{T_i} and f_t is summarized in Table I. The effective collisionality $\nu_{eff} = \nu_{ei}/\omega_{De}$ compares the electron-ion collision frequency ν_{ei} to the curvature drift frequency ω_{De} and can be approximated by $\nu_{eff} = 0.1Rn_eZ_{eff}/T_e^2$ [12]. The normalized gradient R/L_X is defined as $R/L_X = -R\nabla X/X$, where X represents T_e, n_e or T_i. The trapped electron fraction f_t is calculated using the formula derived in [13].

TABLE I: PARAMETER RANGE EXPLORED AT MID-RADIUS, ρ=0.55, IN THE STUDY OF THE IMPACT OF PLASMA TRIANGULARITY ON ELECTRON HEAT TRANSPORT.

T_e [keV]	n_e [10^{19}m^{-3}]	Z_{eff}	T_i [keV]	ν_{eff}
0.9-1.7	1.2-2.8	2.2-5.4	0.25-0.45	0.15-0.9
R/L_{T_e}	R/L_{n_e}	T_e/T_i	R/L_{T_i}	f_t
12-17.5	2.5-5.5	3-5	4-7	0.55-0.56

Before describing the plasma triangularity effect on electron heat transport, the other parameters that strongly influence electron heat transport are identified. A previous study performed at constant plasma shape (δ=+0.2 and κ=1.5) indicates that for TCV EC heated L-mode plasmas, the mid-radius electron heat diffusivity is independent of the normalized temperature gradient R/L_{T_e}, if $R/L_{T_e} > 10$ [11]. In contrast, the electron temperature, the electron density and the effective charge strongly influence the experimental electron heat transport which suggests a dependence of χ_e on the effective collisionality $\nu_{eff} \propto n_eZ_{eff}/T_e^2$. The effective

collisionality does indeed play a major role in the stability of TEM and, as shown by local gyro-fluid linear simulations performed with GLF23 [14], TEM are the dominant micro-instability for the plasmas considered in this study. The range of T_e, n_e and Z_{eff} covered at mid-

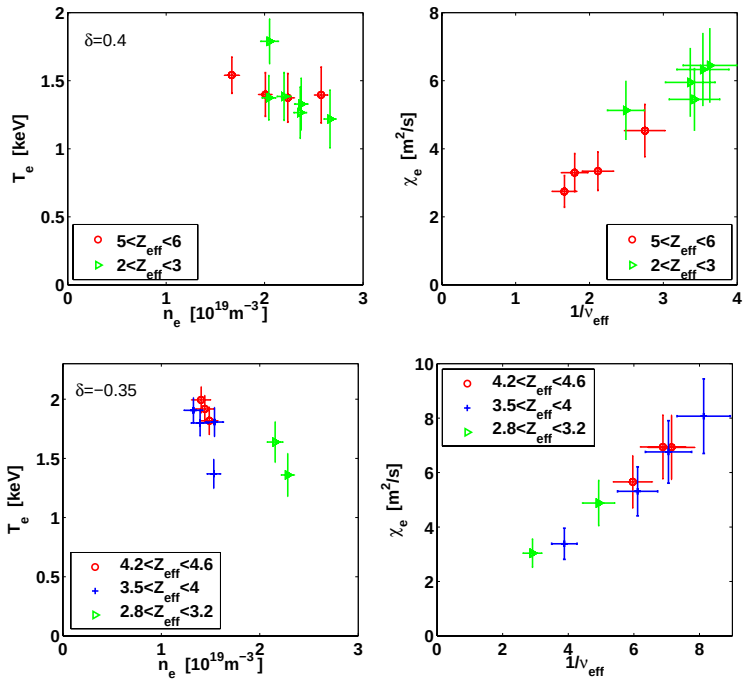

FIG. 3. Range of T_e, n_e and Z_{eff} covered at mid-radius for two plasma triangularities, δ=+0.4 (top plots) and δ=–0.35 (bottom plots). The mid-radius electron heat diffusivity χ_e dependence on T_e, n_e and Z_{eff} may be combined into a unique dependence on the plasma effective collisionality ν_{eff}.

radius together with the electron heat diffusivity as a function of $1/\nu_{eff}$ are shown in FIG. 3 for two plasma triangularities, δ=0.4 and –0.35. As shown in FIG. 3, χ_e not only depends on T_e, n_e and Z_{eff} but this dependence may be cast as a dependence on the plasma effective collisionality. The electron heat transport is shown to significantly decrease towards high effective collisionalities, as would be expected from the TEM dependence on ν_{eff}. The effect of ν_{eff} on electron heat transport has also been demonstrated in ASDEX Upgrade L-mode plasmas [15]. For the plasmas considered in FIG. 3, the normalized temperature gradient values at mid-radius range between 12 and 16, the safety factor and magnetic shear vary by <10% and the normalized density gradient values vary between 1.5 and 4, with no correlation with ν_{eff}. It should be noted that the electron temperature variations obtained at constant ν_{eff} are weak and can not be used to determine whether the electron heat transport depends on T_e solely through ν_{eff} or through ν_{eff} together with a further dependence on T_e, like, for instance, a gyro-Bohm dependence.

The dependence of χ_e on ν_{eff} may now be used to investigate the impact of δ on χ_e. The mid-radius electron heat diffusivity is plotted as a function of $1/\nu_{eff}$ in FIG. 4, for the four plasma triangularities considered in this study. The decrease of χ_e with increasing ν_{eff} is confirmed for each plasma shape and a clear decrease of χ_e with decreasing plasma triangularity is obtained. These results change little with the inclusion of a gyro-Bohm normalization for χ_e. For all the plasmas discharges considered, little MHD mode activity is detected and the sawtooth activity, monitored by soft X-ray diagnostics, has a negligible impact on the mid-radius pressure profile. Previous studies, dedicated to the impact of plasma triangularity on sawteeth [2, 3], show that the sawteeth amplitude and frequency variations are parabolic with δ, with an extremum around δ=–0.2.The potential influence of sawteeth on transport may, therefore, not be invoked

to explain the monotonic decrease of χ_e with decreasing triangularity. The influence of the safety factor variation with δ may also be discarded. Part of the study was performed at con-

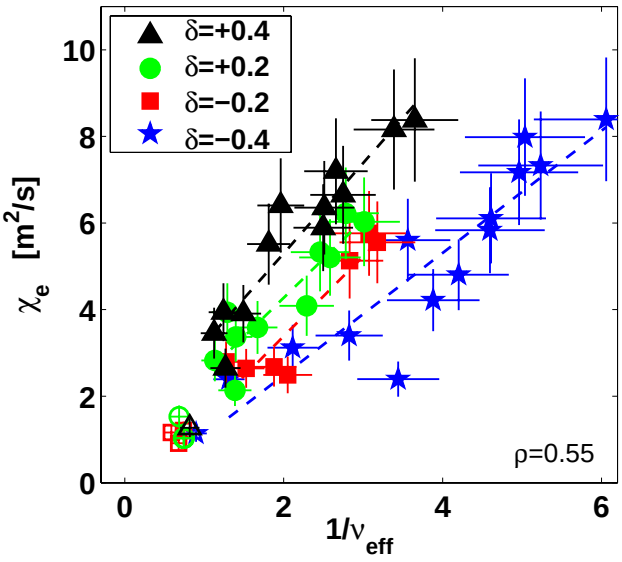

FIG. 4. Decrease of the experimental electron heat diffusivity χ_e with decreasing triangularity δ and increasing plasma collisionality ν_{eff} in EC heated L-mode plasmas (full symbols). In high collisionality ohmic plasmas (open symbols), the effect of plasma triangularity on χ_e is no longer observed.

stant total current, with another part at constant edge safety factor q_{edge}. In the first case, I_p=260κA to within ±5% and q_{edge} varies from 4.2 to 5.6 in the triangularity scan. The q=1 surface radius ρ_1, mainly proportional to the average current density, is also constant to within ±5% and ρ_1=0.3. In the second case, q_{edge}=5.5 to within ±5% and 240<I_p<290kA. The current variation with δ is parabolic with a minimum around δ=–0.2. The q=1 surface radius follows the variations of I_p and ρ_1=0.3 to within ±20%. In both cases, the variation of χ_e with δ and ν_{eff} are similar and the two set of points can not be distinguished in FIG. 4. This does not mean that the electron heat transport does not depend on the safety factor profile, but only that, in the present study, the mid-radius safety factor variations are too small to have a significant impact on χ_e.

For EC heated L-mode plasmas (full symbols in FIG. 4), the electron heat transport decreases with increasing collisionality and decreasing triangularity. For ohmic plasmas (open symbols in FIG. 4) of about the same electron density, the effective collisionality is higher and, as shown in FIG. 4, the triangularity effect on χ_e is no longer observed. This underlines the strong impact of plasma collisionality on electron heat transport and possibly explains why the energy confinement improvement with decreasing triangularity, observed in low collisionality EC heated plasmas [7, 11], is not observed in high collisionality ohmic plasmas [4, 5].

5. TEM dependence on plasma triangularity

In addition to the local gyro-fluid linear simulations (GLF23) showing that TEM are the dominant instability, dedicated global gyro-kinetic colisionless simulations are performed with the linear code LORB5 [16] to investigate the impact of δ on TEM. The triangularity of the last flux surface is varied from δ=–0.3 to δ=+0.5, while the T_e, n_e, T_i, Z_{eff} and current profiles, taken from an experimental case, are kept constant. The plasma equilibrium description is calculated for each triangularity using the Grad-Shafranov solver of MHD equilibria CHEASE [17]. For ρ<0.8, the trapped electron fraction is identical for each triangularity to within ±5%.

For the experimental reference plasma, the C^{6+} ion toroidal velocity, measured by the CXRS diagnostic, is <10km/s across the whole radial profile and the radial electric field is often rather weak in TCV plasmas [18]. In these conditions, the $\vec{E} \times \vec{B}$ stabilization of the TEM is negligible and is therefore not included in the simulations. For all plasma triangularities and toroidal wave numbers n, the simulations indicate that the TEM is the dominant instability and the electron contribution to the total growth rate γ is more than 90%. The growth rate γ, the

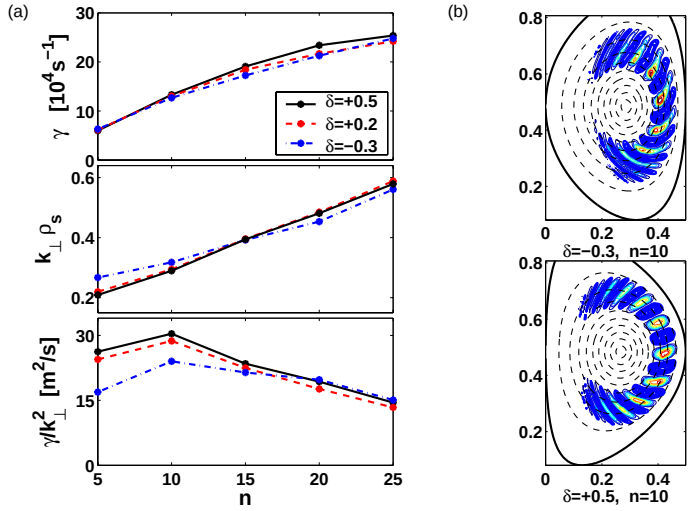

FIG. 5. Global gyro-kinetic linear simulations (LORB5) showing the impact of the plasma triangularity on the TEM properties. Left plots (a): TEM growth rate γ, perpendicular wave vector times the ion Larmor radius $k_\perp\rho_s$ and mixing length transport level $\gamma/k_\perp^2$, for toroidal waves numbers $5<n<25$. Right plots (b) poloidal structure of the n=10 electrostatic potential for δ=–0.3 *and* δ=+0.5.

perpendicular wave vector $k_\perp$ and the mixing length heat diffusivity $\chi_e^{mix}=\gamma/k_\perp^2$ are shown in FIG. 5 as a function of the toroidal wave number. The maximum transport level is obtained for n=10 with the mixing length heat diffusivity decreasing significantly towards negative triangularities for $n\leq10$. The poloidal structure of the electrostatic potential obtained for n=10 is shown in FIG. 5, for δ=–0.3 and δ=0.5. The plasma triangularity has a marked impact on the TEM properties, mainly $k_\perp$ increases with decreasing δ for low n values, which could possibly explain the decrease of χ_e towards negative δ observed in the experiments.

6. Conclusions

The electron heat transport has been studied in L-mode plasmas in the presence of EC heating power deposited in the plasma core. In these conditions, it is shown that the electron heat diffusivity dependence on the electron temperature, electron density and effective charge can be combined as a dependence on the plasma effective collisionality. The effect of plasma triangularity on the electron heat diffusivity is demonstrated for a wide range of plasma collisonalities. The electron heat transport is shown to decrease significantly with increasing collisionality and decreasing triangularity. Local gyro-fluid (GLF23) and global gyro-kinetic (LORB5) simulations predict that the micro-instabilities potentially responsible for anomalous heat transport in these EC heated plasmas are the trapped electron modes (TEM). The dependence of the TEM growth rate and perpendicular wave vector on plasma triangularity observed in global simulations could be at the origin of the experimental decrease of χ_e with decreasing triangularities. The decrease of χ_e, occurring in the plasma bulk, has a strong impact on the electron energy confinement. In contrast to low collisionality EC heated L-mode plasmas, the electron heat diffusivity and the energy confinement no longer depend on the

plasma triangularity in high collisionality ohmic L-mode plasmas. This underlines the prominent role of plasma collisionality in electron heat transport.

In high collisionality H-mode plasmas, as the triangularity is increased, the increase in the edge stability and pedestal height results in an increase of the energy confinement time [19, 20]. At low collisionality, however, the effect of the pedestal would compete with an increase of the core electron heat transport with triangularity similar to that observed in L-mode plasmas. The overall dependence of the energy confinement on the plasma triangularity remains, therefore, an open question that requires now a study of the role of plasma shape on electron heat transport in low collisionality H-mode plasmas.

It is a pleasure to acknowledge the competent support of the entire TCV team.
Global simulations were performed on the parallel server SGI Origin 3800 and the Linux cluster PLEIADES of the Ecole Polytechnique Fédérale de Lausanne.
This work was partially supported by the Swiss National Science Foundation.

[1] HOFMANN, F., et al., "Experimental and Theoretical Stability Limits of Highly Elongated Tokamak Plasmas", Phys. Rev. Lett. **81** (1998) 2918.
[2] REIMERDES, H., et al., "Effect of triangular and elongated plasma shape on the sawtooth instability", Plasma Phys. Control. Fusion **42** (2000) 629.
[3] MARTYNOV, A., et al., "The stability of the ideal internal kink mode in realistic tokamak geometry", Plasma Phys. Control. Fusion **47** (2005) 1743.
[4] MORET, J.-M., et al., "Influence of Plasma Shape on Transport in the TCV Tokamak", Phys. Rev. Lett. **79** (1997) 2057.
[5] WEISEN, H., et al., "Effect of plasma shape on confinement and MHD behaviour in the TCV tokamak", Nucl. Fusion **37** (1997) 1741.
[6] HOFMANN, F., et al., "Stability and energy confinement of highly elongated plasmas in TCV", Plasma Phys. Control. Fusion **43** (2001) A161.
[7] POCHELON, A., et al., "Energy confinement and MHD activity in shaped TCV plasmas with localized electron cyclotron heating", Nucl. Fusion **39** (1999) 1807.
[8] MATSUDA, K., et al., "Ray Tracing Study of the Electron Cyclotron Current Drive in DIII-D Using 60GHz", IEEE Trans. Plasma Sci. **17** (1989) 6.
[9] ANGIONI, C., et al., "Effects of localized electron heating and current drive on the sawtooth period", Nucl. Fusion **43** (2003) 455.
[10] BOUCHER, D., REBUT, P.H., Proc. Tech. Committee Meeting on Advances in Simulation and Modelling of Thermonuclear Plasmas Montreal, 1992, IAEA, Vienna (1993), p. 142.
[11] CAMENEN, Y., et al., "Electron heat transport in shaped TCV L-mode plasmas", Plasma Phys. Control. Fusion **47** (2005) 1971.
[12] ANGIONI, C., et al., "Theory-based modelling of particle transport in ASDEX Upgrade H-mode plasmas: density peaking, anomalous pinch and collisionality", Phys. Plasmas **10** (2003) 3225.
[13] LIN-LIU, Y.R., MILLER, R.L., "Upper and lower bounds of the effective trapped particle fraction in general tokamak equilibria", Phys. Plasmas **2** (1995) 1666.
[14] WALTZ, R.E., et al., "A gyro-Landau-fluid transport model", Phys. Plasmas **4** (1997) 2482.
[15] RYTER, F., et al., "Experimental Study of Trapped-Electron-Mode Properties in Tokamaks: Threshold and Stabilization by Collisions", Phys. Rev. Lett. **95** (2005) 085001.
[16] BOTTINO, A., et al., "Simulations of global electrostatic microinstabilities in ASDEX Upgrade discharges", Phys. Plasmas **11** (2004) 198.
[17] LÜTJENS, H., et al., "The CHEASE code for toroidal MHD equilibria", Comput. Phys. Commun. **97** (1996) 219.
[18] SCARABOSIO, A., et al., "Toroidal plasma rotation in the TCV tokamak", Plasma Phys. Control. Fusion **48** (2006) 663.
[19] STOBER, J., et al., "Effect of triangularity on confinement, density limit and profile stiffness of H-modes on ASDEX Upgrade", Plasma Phys. Control. Fusion **42** (2000) A211.
[20] SAIBENE, G., et al., "Improved performance of ELMy H-modes at high density by plasma shaping in JET", Plasma Phys. Control. Fusion **44** (2002) 1769.